Cellular and Humoral Immune Responses in Mice Immunized with Vaccinia Virus Expressing the SARS-CoV-2 Spike Protein

The Journal of Immunology

Jake C. Harbour, Zoe L. Lyski, John B. Schell, Archana Thomas, William B. Messer, Mark K. Slifka and Jeffrey C. Nolz

---

References   This article **cites 57 articles**, 15 of which you can access for free at:
http://www.jimmunol.org/content/206/11/2596.full#ref-list-1

Why *The JI*? Submit online.

- **Rapid Reviews! 30 days*** from submission to initial decision

- **No Triage!** Every submission reviewed by practicing scientists

- **Fast Publication!** 4 weeks from acceptance to publication

average

Subscription   Information about subscribing to *The Journal of Immunology* is online at:
http://jimmunol.org/subscription

Permissions   Submit copyright permission requests at:
http://www.aai.org/About/Publications/JI/copyright.html

Email Alerts   Receive free email-alerts when new articles cite this article. Sign up at:
http://jimmunol.org/alerts

Cellular and Humoral Immune Responses in Mice Immunized with Vaccinia Virus Expressing the SARS-CoV-2 Spike Protein

Jake C. Harbour,* Zoe L. Lyski,*[,1] John B. Schell,[†,1] Archana Thomas,[‡,1] William B. Messer,*[,§,¶] Mark K. Slifka,[‡] and Jeffrey C. Nolz*[,‖,#]

The COVID-19 pandemic is a global health emergency, and the development of a successful vaccine will ultimately be required to prevent the continued spread and seasonal recurrence of this disease within the human population. However, very little is known about either the quality of the adaptive immune response or the viral Ag targets that will be necessary to prevent the spread of the infection. In this study, we generated recombinant Vaccinia virus expressing the full-length spike protein from SARS-CoV-2 (VacV-S) to evaluate the cellular and humoral immune response mounted against this viral Ag in mice. Both CD8+ and CD4+ T cells specific to the SARS-CoV-2 spike protein underwent robust expansion, contraction, and persisted for at least 40 d following a single immunization with VacV-S. Vaccination also caused the rapid emergence of spike-specific IgG-neutralizing Abs. Interestingly, both the cellular and humoral immune responses strongly targeted the S1 domain of spike following VacV-S immunization. Notably, immunization with VacV-expressing spike conjugated to the MHC class II invariant chain, a strategy previously reported by us and others to enhance the immunogenicity of antigenic peptides, did not promote stronger spike-specific T cell or Ab responses in vivo. Overall, these findings demonstrate that an immunization approach using VacV or attenuated versions of VacV expressing the native, full-length SARS-CoV-2 spike protein could be used for further vaccine development to prevent the spread of COVID-19. *The Journal of Immunology*, 2021, 206: 2596–2604.

C oronavirus infectious disease of 2019 (COVID-19) is a highly contagious, often deadly respiratory illness that is caused by the novel betacoronavirus severe acute respiratory syndrome coronavirus 2 (SARS-CoV-2) (1, 2). Unlike other coronaviruses such as human coronavirus OC43, HKU, and 229E that are endemic within the human population and typically cause only mild disease (i.e., the common cold), SARS-CoV-2, as well as its close relatives SARS-CoV-1 and Middle East respiratory syndrome coronavirus, are highly pathogenic coronaviruses that have emerged within the last two decades, causing significant illness with high mortality rates (3, 4). Because the vast majority of the global human population has not been previously exposed to any of these closely related novel betacoronaviruses, understanding the level of adaptive immunity required to protect an individual from infection will be necessary for evaluating long-term vaccine efficacy and ultimately achieving "herd immunity" (5). However, the magnitude and breadth of the adaptive immune response, as well as the viral Ags being targeted, following either natural infection or after different types of vaccinations, remain largely unknown.

SARS-CoV-2, SARS-CoV-1, and Middle East respiratory syndrome coronavirus are enveloped, positive-sense ssRNA viruses of the family *Coronaviridae* and are comprised of four structural proteins: spike, envelope, membrane, and nucleocapsid (6). Among the different structural proteins, spike is responsible for cellular invasion, where the N-terminal S1 domain facilitates attachment and the C-terminal S2 domain then initiates viral fusion with the cell membrane. The receptor for spike for all three novel betacoronaviruses is angiotensin-converting enzyme 2 (ACE2), and the receptor binding domain (RBD) for ACE2 lies within the S1 domain of spike (7). Because the S1 domain of spike mediates the initial attachment of the virus to a cell expressing ACE2, there has been considerable interest in identifying Abs against spike that can effectively neutralize SARS-CoV-2 in vivo (8–12). Both cytotoxic and helper T cell responses against all of the structural proteins of SARS-CoV-2, including spike, have been documented in humans (13–15), but how effective spike-specific (S-specific) T cell populations are at identifying and eliminating cells infected with SARS-CoV-2 remains to be fully determined (16). Nevertheless, adaptive immune responses

---

*Department of Molecular Microbiology and Immunology, Oregon Health & Science University, Portland, OR; †Vaccine and Gene Therapy Institute, Oregon Health & Science University, Beaverton, OR; ‡Oregon National Primate Research Center, Oregon Health & Science University, Beaverton, OR; §Department of Medicine, Division of Infectious Diseases, Oregon Health & Science University, Portland, OR; ¶Program in Epidemiology, Oregon Health & Science University-Portland State University School of Public Health, Oregon Health & Science University, Portland, OR; ‖Department of Cell, Developmental and Cancer Biology, Oregon Health & Science University, Portland, OR; and #Department of Radiation Medicine, Oregon Health & Science University, Portland, OR

[1]Z.L.L., J.B.S., and A.T. contributed equally.

ORCIDs: 0000-0003-2485-3932 (J.C.H.); 0000-0003-3631-8072 (Z.L.L.); 0000-0001-6707-7051 (J.B.S.); 0000-0003-4701-7419 (J.C.N.).

against the spike protein following vaccination, both cellular and humoral, warrants further investigation using experimental model systems, which could provide valuable clues about identifying strategies to promote robust protective immunity to prevent the spread of COVID-19.

Vaccinia virus (VacV) is a highly immunogenic poxvirus, and its use as a vaccine was ultimately responsible for the eradication of smallpox from the planet (17, 18). Studies in humans receiving the smallpox vaccine demonstrate the durability and longevity of immunity mounted against this virus. In fact, Abs against VacV appear to persist for life, and cellular immunity can be identified in most individuals, even decades after vaccination (19–22). Because of that success, recombinant versions of VacV or the highly attenuated modified VacV Ankara (MVA) have been and are currently being pursued as subunit vaccine candidates for a number of other infectious diseases, including Middle East respiratory syndrome (23–26). Furthermore, MVA expressing full-length spike from either SARS-CoV-1 or SARS-CoV-2 have also been tested experimentally in animal models (27–30). Those studies found that vaccination results in the production of S-specific Abs that provide protection against both SARS-CoV-1 and SARS-CoV-2 infections. Whether or not S-specific cytotoxic or helper T cells generated by these types of immunization strategies are durable and/or able to provide protection against SARS-CoV-2 infection warrants further investigation.

In this study, we generated recombinant VacV expressing the full-length SARS-CoV-2 spike protein (VacV-S) to quantify the magnitude and kinetics of the cellular and humoral immune responses against this viral Ag in immunized animals. We found that immunization with VacV-S generated a robust S-specific CD8$^+$ T cell response, a modest but readily detectable S-specific CD4$^+$ T cell response, and high titers of S-specific IgG-neutralizing Abs. Interestingly, we found that both CD8$^+$ and CD4$^+$ T cells, as well as IgG-neutralizing Abs, targeted primarily the S1 domain of spike. Notably, we also found that conjugating the MHC class II (MHC-II) invariant chain (Ii) to the C terminus of spike, a strategy previously shown to enhance the immunogenicity of peptides (31–33), caused degradation of the viral Ag and did not promote stronger cellular or humoral immune responses against spike in vivo. Overall, our findings shows that the full-length spike protein is highly immunogenic, and delivering this gene using recombinant viral vectors could be a highly efficacious strategy to promote strong cellular and humoral immunity against SARS-CoV-2.

Materials and Methods

Generation of recombinant VacV-expressing SARS-CoV-2 spike

Recombinant VacV expressing the full-length spike gene from SARS-CoV-2 and spike conjugated to Ii were generated by homologous recombination targeting the thymidine kinase (*tk*) gene of VacV, as previously described (34). A codon-optimized version of spike (GenScript) was PCR amplified using oligonucleotides that would introduce SalI and KpnI restriction sites at the 5′ and 3′ end of the PCR product, respectively, and subsequently cloned into the pSC11 plasmid. To generate spike conjugated to Ii, full-length spike was PCR amplified and cloned as described above with the exception that the 3′ oligonucleotide resulted in the loss of the stop codon. The MHC-II Ii was PCR amplified using oligonucleotides to introduce an in-frame 5′ KpnI and 3′ NotI restriction sites and subsequently cloned into pSC11-spike (no stop) to generated pSC11-spike-Ii. Homologous recombination was performed in *tk*$^{-/-}$ 143B cells by infecting cells in a 12-well plate with 5 × 10^5 PFU VacV-WR (BEI Resources) followed by transfection with 1 ug of pSC11-spike or pSC11-spike-Ii plasmid. The resulting cell lysates were then used to infect *tk*$^{-/-}$ 143B cells in the presence of BrdU and 4% X-gal. After three rounds of plaque purification in the presence of BrdU, individual viral plaques were screened by DNA sequencing, and successfully recombined viruses were expanded and quantified using BSC-40 cells and standard procedures. VacV-Ii-gp$_{61-80}$ has been previously described (32).

Immunoblotting

BSC-40 cells were grown to confluency in a 12-well plate and infected with VacV, VacV-S, VacV-S-Ii, or VacV-Ii-gp$_{61-80}$ (multiplicity of infection [MOI] = 1.0). Twenty-four hours postinfection, cells were lysed in a 1% Igepal lysis buffer (20 mM HEPES [pH 7.9], 100 mM NaCl, 5 mM EDTA, 1% Igepal, 1 mM PMSF, 10 μg/ml leupeptin, and 5 μg/ml aprotinin). Following clarification by centrifugation, equal amounts of protein were resolved by SDS-PAGE on a 7.5% or 4–20% acrylamide gel (Bio-Rad Laboratories) and transferred to Immobilin P membranes (MilliporeSigma). Expression of spike was detected using a rabbit polyclonal anti-sera against the S1 domain (catalog [Cat] no. GTX135356, GeneTex) or a mouse mAb against the S2 domain (clone IA9, Cat no. GTX632604, GeneTex) at a 1:1000 dilution in 2% BSA/TBS incubated overnight at 4°C and goat anti-rabbit HRP or goat anti-mouse HRP (Jackson ImmunoResearch Laboratories). Expression of MHC-II Ii (CD74) was detected using a rat mAb (clone In1; BioLegend) at a 1:1000 dilution in 2% BSA/TBS incubated overnight at 4°C and goat anti-rat HRP (Santa Cruz Biotechnology). Luminescent images were acquired using an Image Quant LAS 400 (GE Healthcare) scanner.

Mice and infections

C57BL/6N mice were purchased from National Cancer Institute/Charles River Laboratories and used for experiments at 6–8 wk of age. Mice were immunized with 10^7 PFU of VacV, VacV-S, or VacV-S-Ii in 200 μl of sterile PBS and delivered i.v. by tail vein injection.

Ex vivo peptide stimulation and intracellular cytokine stain

Peptide pools consisting primarily of 15-mer sequences with 11 aa overlap covering the entire SARS-CoV-2 spike protein were purchased from Miltenyi Biotec. The S1 pool consists of overlapping peptides covering amino acids 1–692 of spike (Cat no. 130-127-041). To generate a peptide pool consisting of primarily the S2 domain, we combined peptide pools "S" (Cat no. 130-126-700) and "S+" (Cat no. 130-127-311). This combination of peptide pools (S and S+) covered the entire S2 domain as well as three short segments of the S1 domain (amino acids 304–338, 421–475, and 492–519). Lyophilized peptides were resuspended in 20% DMSO in sterile water and diluted to a final concentration of ~0.6 nmol per peptide for cell stimulation, according to the manufacturer's protocol. B8R$_{20-27}$ peptide was purchased from BioSynthesis. Peripheral blood leukocytes or splenocytes were stimulated with S-specific peptides or B8R$_{20-27}$ for 5 h at 37°C in the presence of brefeldin A (BioLegend). Cells were then stained for surface Ags in 1% FCS/PBS for 15 min, washed, and fixed with BD Cytofix/Cytoperm solution for 15 min at 4°C. Intracellular stain for IFN-γ or TNF was performed in Perm/Wash buffer for 20 min at 4°C. Cells were then washed and resuspended in 1% FCS/PBS prior to FACS analysis.

Abs and flow cytometry

The following fluorescently labeled Abs and appropriate isotype controls (all from BioLegend) were used in this study: CD8α (53-6.7), CD4 (GK1.5), IFN-γ (XMG1.2), TNF (MP6-XT22), and CD44 (IM7). Data were collected on a BD Symphony in the Oregon Health & Science University Flow Cytometry Core facility. Data were analyzed using FlowJo software (version 9.9.6).

Quantification of spike-specific Abs

To quantify Abs against the full-length spike protein at different time points following immunization, 96-well ELISA plates (Cat no. 3590, Corning) were coated with 100 μl of recombinant SARS-CoV-2 full-length spike protein (Cat no. 40589-V08B1, Sino Biological) at a concentration of 1 μg/ml prepared in PBS, and the plates were incubated overnight at 4°C. Coating Ag was removed, and plates were washed once with PBS containing 0.05% Tween (wash buffer) and blocked for 1 h at room temperature (RT) with 5% milk prepared in PBS containing 0.05% Tween (dilution buffer). Then, 100 μl of 1:30 dilution of serum (in dilution buffer) was added to each well. Serum samples were serially 3-fold diluted in dilution buffer. Plates were incubated at RT for 1 h. The plates were washed three times with wash buffer, and 100 μl of 1:4000 dilution of anti-mouse IgG-HRP (Cat no. 115-035-071, Jackson ImmunoResearch Laboratories) detection Ab was added and incubated at RT for 1 h. To quantify Abs against S1, S2, and RBD, 96-well ELISA plates (Cat#3590, Corning) were coated with 100 μl of each Ag, recombinant RBD protein (Cat no. 230-30162-100, RayBiotech), recombinant subunit 1 protein (Cat no. 40591-V08H, Sino Biological), and recombinant S2 (Cat no. 40150-v08B3, Sino Biological) at a concentration of 1 μg/ml prepared in PBS, and the plates were incubated overnight at 4°C. Coating Ag was removed, and plates were washed once with PBS containing 0.05% Tween (wash buffer) and blocked for 1 h at RT with 5% milk prepared in PBS containing 0.05% Tween (dilution buffer). Then, 100 μl of 1:100

dilution of serum (in dilution buffer) was added to each well. Serum samples were serially 2-fold diluted in dilution buffer and plates were incubated at RT for 1 h. The plates were washed three times with wash buffer, and 100 μl of 1:2000 dilution of anti-mouse IgG-HRP (Cat no. 405306, BioLegend) detection Ab was added and incubated at RT for 1 h. For all analyses, the plates were washed three times, 100 μl of colorimetric detection reagent containing 0.4 mg/ml o-phenylenediamine and 0.01% hydrogen peroxide in 0.05 M citrate buffer (pH 5) were added, and the reaction was stopped after 20 min by the addition of 100 μl 1 M HCl. OD at 492 nm was measured using a plate reader. Ab titers (ELISA units) were determined by log–log transformation of the linear portion of the curve after background subtraction, with 0.1 OD units as the end point used to convert the final values.

Quantification of neutralization Abs

A VSVΔG-luciferase encoding plasmid was generated by replacing the glycoprotein gene with the firefly luciferase gene using MluI and NheI restriction sites present in the pVSV-XN2 genomic plasmid. Viral stocks were recovered as described previously (35, 36). The SARS-CoV-2 spike (S) encoding pUC57-2019-nCoV-S plasmid (GenScript) was used to generate an S PCR fragment lacking the last 21 aa of the C terminus (37). This SARS-CoV-2 S gene fragment was cloned into the pND-1 expression plasmid and used to pseudotype the VSVΔG-luciferase particles outlined in Ref. 38. The resulting viruses were quantified using VeroE6 cells and used in luciferase assays at a concentration that gave $3–4 \times 10^5$ relative light units per well. For the neutralization assay, VeroE6 cells were plated at a concentration of 2×10^4 per well in a 96-well black, clear-bottom plate (Corning) 1 d prior to infection. The neutralization capacity of the sera was determined by coincubating pseudotyped viruses with 2-fold serial dilutions of immune sera with serum-free media in triplicate for 30 min at 37°C in a humidified incubator. Inocula were then transferred to VeroE6 cells and incubated overnight. Cells were lysed and developed using the Cell Culture Lysis and Luciferase Assay System reagents (Promega), following the manufacturer's recommended protocols. Resulting relative light units were quantified using the GloMax Navigator

microplate luminometer (Promega). IC_{50} was calculated using Prism Software (GraphPad), as described in Ref. 39.

Statistical analyses

Statistics were calculated using Prism Software (GraphPad) using paired or unpaired Student t tests or ANOVA with Tukey correction for multiple comparisons.

Results

Vaccination with VacV expressing the full-length spike protein from SARS-CoV-2 activates both CD8+ and CD4+ S-specific T cells

We generated recombinant tk-VacV expressing a human codon-optimized version of the full-length, SARS-CoV-2 spike protein downstream of the p7.5 promoter (see Materials and Methods for details) to determine if delivery of this viral Ag by VacV would stimulate activation of the adaptive immune system. Expression of the SARS-CoV-2 spike protein by VacV-S was confirmed in vitro where, compared with a control VacV infection, expression of the full-length spike protein could be identified with the predicted molecular mass of ∼180–200 kDa (Fig. 1A). After confirming expression of spike by VacV-S, we next asked whether VacV-S would activate S-specific T cells in vivo. We vaccinated naive C57BL/6 mice with 10^7 PFU of VacV-S delivered i.v., and on day 7 postvaccination, PBLs were stimulated with overlapping peptide pools (see Materials and Methods for details) composed of primarily the S1 or S2 domains of SARS-CoV-2 spike protein. CD44 is highly expressed by both effector and memory T cells (40); thus, we analyzed expression of the cytokine IFN-γ within the CD44Hi compartment of both CD8+ and CD4+ T cells by intracellular stain following peptide stimulation. Compared with the no peptide control, we observed a robust S-
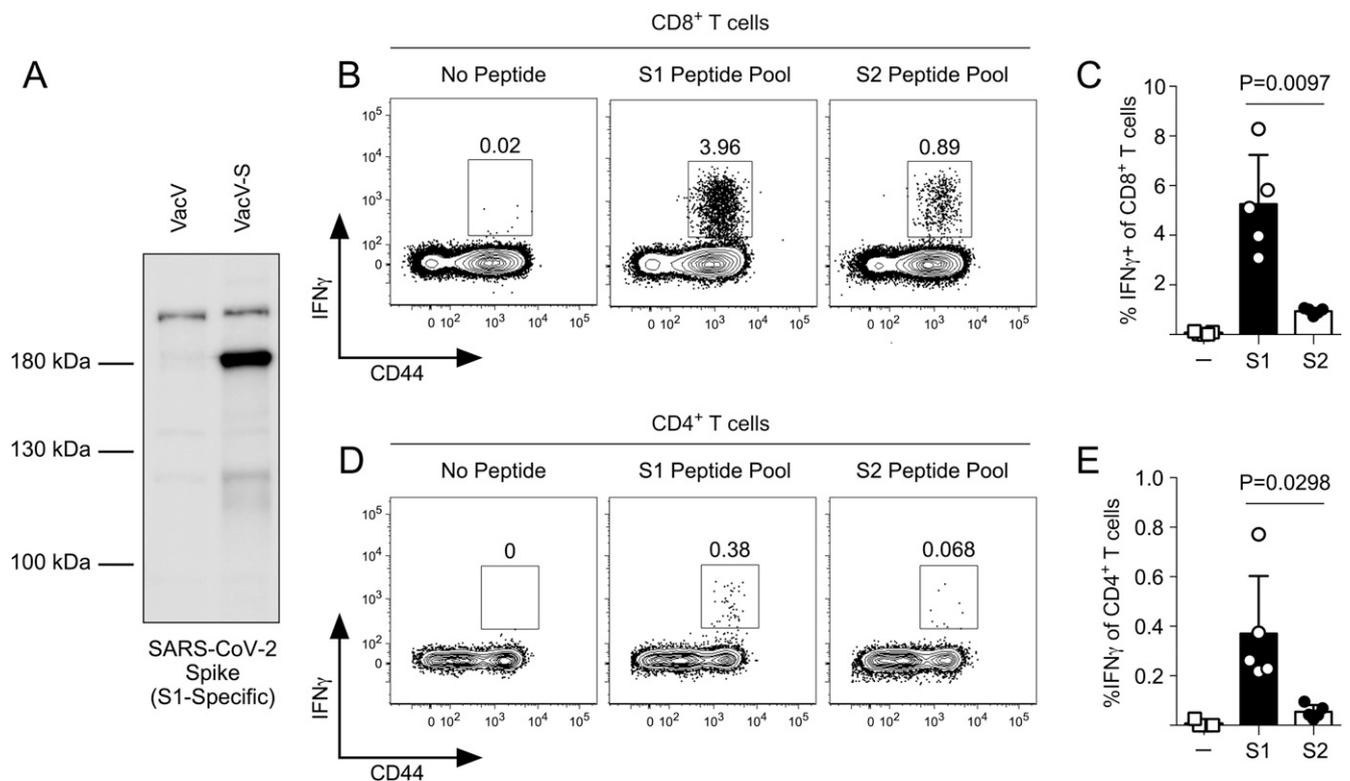
FIGURE 1. Vaccination with VacV-S activates CD8+ and CD4+ T cells in vivo. (**A**) BSC-40 cells were infected with VacV or VacV-S (MOI = 1.0). Twenty-four hours later, expression of spike was analyzed by immunoblot. (**B**) Naive C57BL/6 mice were vaccinated intravenously with 1×10^7 PFU of VacV-S. On day 7 postvaccination, peripheral blood leukocytes were stimulated with either S1 or S2 domain peptide pools, and expression of IFN-γ by CD8+ T cells was detected by intracellular stain. (**C**) Quantification of (B). (**D**) Same as (B) except expression of IFN-γ by CD4+ T cells was detected by intracellular stain. (**E**) Quantification of (D). Error bars indicate SD of the mean, and data are representative of two independent experiments using five mice per group.
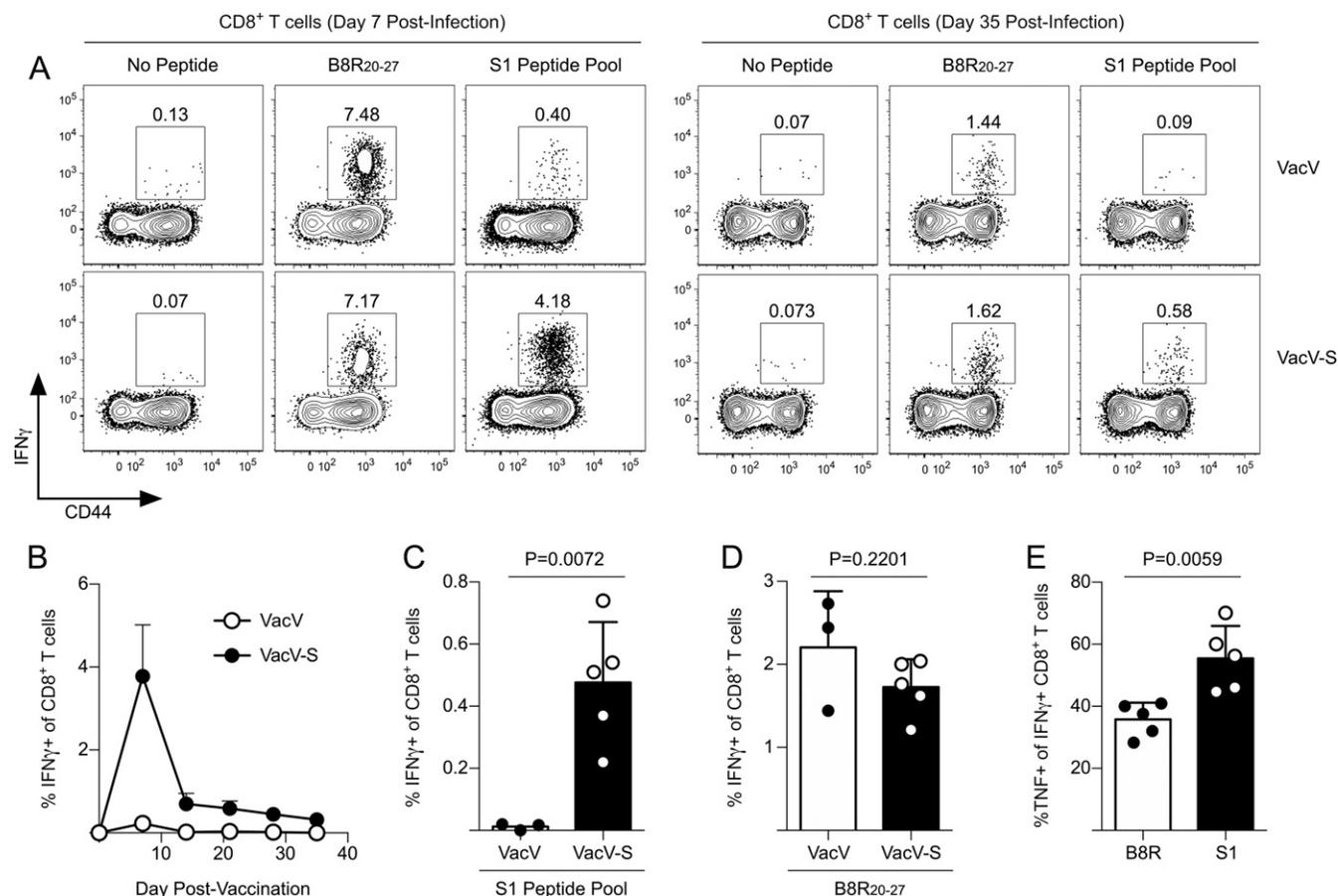
FIGURE 2. Kinetics of the CD8$^+$ T cell response in the circulation following vaccination with VacV-S. (**A**) Naive C57BL/6 mice were immunized with 1×10^7 PFU of VacV or VacV-S. Peripheral blood leukocytes were stimulated with B8R$_{20-27}$ or S1 peptide pool, and expression of IFN-γ by CD8$^+$ T cells was analyzed by intracellular stain. Representative data from days 7 and 35 postvaccination are shown. (**B**) Weekly quantification of data from (A). (**C**) Percentage of CD8$^+$ T cells producing IFN-γ in the blood following stimulation with S1 peptides on day 35 postvaccination. (**D**) Percentage of CD8$^+$ T cells producing IFN-γ in the blood following stimulation with B8R$_{20-27}$ peptide on day 35 postvaccination. (**E**) Percentage of IFN-γ$^+$ T cells from (C) and (D) that coexpress TNF after peptide stimulation. Error bars indicate SD of the mean, and data are representative of three independent experiments using three to five mice per group.

specific CD8$^+$ T cell response against both the S1 and S2 domains of spike (Fig. 1B, 1C). Interestingly, we consistently found that more CD8$^+$ T cells produced IFN-γ when stimulated with S1 peptides compared with S2 peptides, which suggests that this portion of the protein either undergoes better Ag presentation using this immunization strategy or that more immunodominant epitopes in C57BL/6 mice are found within this domain. S-specific CD4$^+$ T cells producing IFN-γ also expanded following vaccination (Fig. 1D, 1E), although at ~10 times lower magnitude compared with CD8$^+$ T cells, but like CD8$^+$ T cells, the majority of the response also targeted the S1 domain of spike. Thus, these data demonstrate that VacV expressing the full-length spike protein from SARS-CoV-2 stimulated strong activation of both CD8$^+$ and CD4$^+$ T cells, with the majority of both responses targeting the S1 rather than the S2 domain of the protein.

S1-specific T cells persist following vaccination with VacV-S

Because we found that both CD8$^+$ and CD4$^+$ S-specific T cells rapidly expanded following VacV-S vaccination, we next determined whether these T cells would persist following contraction. To test this, mice were vaccinated with either VacV (negative control) or VacV-S, and the S1-specific CD8$^+$ T cell response in the circulation was monitored longitudinally using ex vivo S1 peptide pool stimulation followed by intracellular cytokine staining for IFN-γ.

We also included an analysis of the immunodominant epitope found within the VacV genome (B8R$_{20-27}$ presented by H2-K^b in C57BL/6 mice) to compare the magnitude of the S-specific response to this well-defined, virus-specific CD8$^+$ T cell population. Expansion of B8R-specific CD8$^+$ T cells was robust and similar following VacV and VacV-S immunization, demonstrating that both viral immunizations were equally effective at generating an immune response in vivo (Fig. 2A). In VacV-S–vaccinated animals, S1-specific CD8$^+$ T cell expansion peaked on day 7 postvaccination, and the magnitude of the response was nearly 50% the size of the CD8$^+$ T cell population specific for the B8R$_{20-27}$ peptide (Fig. 2A). Notably, we consistently found a small percentage of IFN-γ–producing CD8$^+$ T cells from VacV-immunized animals when stimulated with S1 peptides compared with the unstimulated control on day 7 postinfection ($p = 0.0093$), suggesting that some VacV-specific CD8$^+$ T cells may cross-react with epitopes found within the S1 domain of SARS-CoV-2 spike. S1-specific CD8$^+$ T cells contracted by day 14 but formed a stable population that could be detected by ex vivo peptide stimulation at day 35 postvaccination (Fig. 2A–C), whereas the percentage of B8R-specific CD8$^+$ T cells was the same between both groups (Fig. 2D). In addition, S1-specific CD8$^+$ T cells also exhibited features of polyfunctionality as coexpression of TNF by IFN-γ$^+$ T cells was found to be slightly higher in S1-specific compared with B8R-specific CD8$^+$ T cells (Fig. 2E). Like CD8$^+$ T

cells, expansion of S1-specific CD4$^+$ T cells peaked on day 7 postvaccination but continued to contract in the circulation until they were no longer detectable by ex vivo S1 peptide pool stimulation on day 35 postvaccination (Fig. 3A, 3B). However, both CD8$^+$ and CD4$^+$ T cells producing IFN-γ could be identified in the spleen following stimulation with S1 peptides at day 40 postimmunization and remained CD44^{Hi}, a commonly used marker to identify memory T cells (Fig. 4A–D). Thus, these data demonstrate that S1-specific CD8$^+$ and CD4$^+$ T cells persist following vaccination with VacV-S and that S1-specific CD4$^+$ T cells appear to be enriched in the spleen compared with the blood.

Spike-specific IgG-neutralizing Abs are generated following vaccination with VacV-S

Because we found that immunization with VacV-S caused both CD8$^+$ and CD4$^+$ T cells to become activated, we next measured whether immunization also resulted in the generation of S-specific IgG Abs. IgG Abs that bound to the full-length spike protein formed by day 14 postvaccination and Ab levels remained stable in the serum through day 35 postvaccination (Fig. 5A). Experimental evidence suggests that Abs targeting the S1 N terminus or RBD are most effective at preventing SARS-CoV-2 infection (8); thus, we next tested whether S-specific IgG Abs were generated against either the S1, S2, and/or the RBD domains of spike following VacV-S immunization (Fig. 5B–E). Abs against both the S1 and S2 domain were readily detected in immune sera, although Ab titers specific for the S2 domain appeared to be ~10-fold less than those that reacted to the S1 domain using this assay (Fig. 5E). We also detected high titers of RBD-specific IgG Abs in mice immunized with VacV-S compared with serum from controls. In agreement with these data demonstrating a strong humoral immune response against the S1 domain of spike, including the RBD, serum from VacV-S–immunized animals prevented infection of VeroE6 cells by pseudotyped vesicular stomatitis virus (VSV) expressing SARS-CoV-2 spike (Fig. 5F). Serum from all animals vaccinated with VacV-S completely blocked S-mediated VSV entry at the lower serum dilutions tested (between 1:200–800), and 50% viral neutralization (IC$_{50}$) occurred at a dilution factor of >10^3 (Fig. 5G). Overall, these data show that immunization with VacV-S results in the rapid development of S-specific IgG-neutralizing Abs.
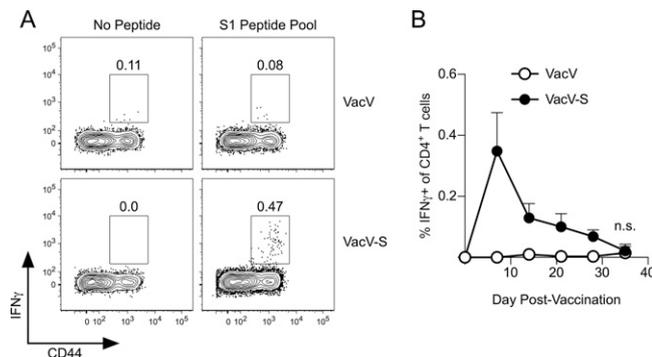

FIGURE 3. Kinetics of the CD4$^+$ T cell response in the circulation following vaccination with VacV-S. (**A**) Naive C57BL/6 mice were immunized with 1×10^7 PFU of VacV or VacV-S. Peripheral blood leukocytes were stimulated with S1 peptide pool, and expression of IFN-γ by CD4$^+$ T cells was analyzed by intracellular stain on day 7 postvaccination. (**B**) Weekly quantification of data from (A) through day 35 postvaccination. Error bars indicate SD of the mean, and data are representative of three independent experiments using three to five mice per group.
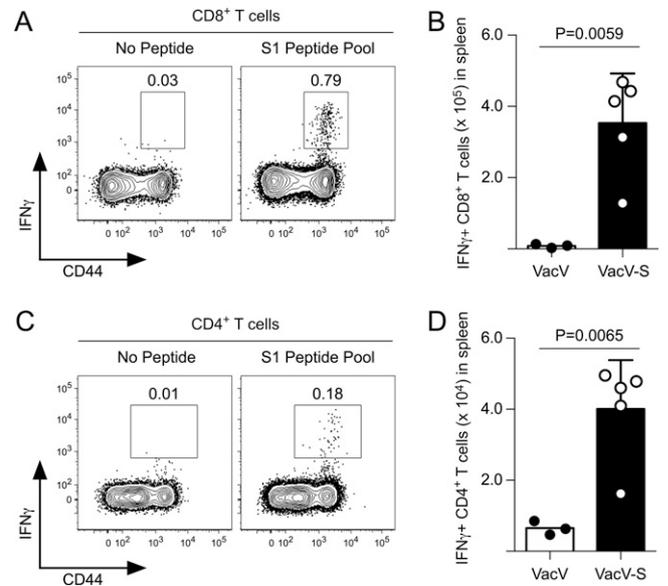
FIGURE 4. S1-specific CD8$^+$ and CD4$^+$ T cells are detected in the spleen 40 d after vaccination with VacV-S. (**A**) Naive C57BL/6 mice were immunized with 1×10^7 PFU of VacV-S. On day 40 postvaccination, splenocytes were stimulated with S1 peptides, and expression of IFN-γ by CD8$^+$ T cells was detected by intracellular stain. (**B**) Quantification of (A) comparing vaccination with VacV (negative control) and VacV-S. (**C** and **D**) Same as (A) and (B) except CD4$^+$ T cells were analyzed. Error bars indicate SD of the mean, and data are representative of two independent experiments using three to five mice per group.

VacV-expressing spike conjugated to the MHC-II Ii does not enhance cellular or humoral immune responses in vivo

We have previously reported that conjugating the MHC-II Ii to immunogenic peptides expressed by VacV resulted in stronger activation of Ag-specific CD4$^+$ T cells in vivo (32). To determine if this also held true using a full-length, >1200 aa transmembrane viral Ag rather than a defined MHC-II restricted peptide, we generated VacV that expressed the full-length spike protein that contained the MHC-II Ii conjugated to its C terminus (VacV-S-Ii). Ii is a type II transmembrane protein with a short N-terminal intracellular domain and an extracellular C-terminal domain that binds directly to MHC-II (41). Because spike is a type I transmembrane protein, we predicted that VacV-S-Ii would produce a chimeric Ag in which the N terminus of spike and the C terminus of Ii would become extracellular and the spike C-terminal and Ii N-terminal intracellular domains would be physically connected. However, immunoblot analysis revealed that unlike the full-length, native version of spike (Fig. 1A), we were unable to detect expression of full-length S-Ii in vitro. Rather, we observed smaller S1-reactive proteins between 55 and 100 kDa in size (Fig. 6A). An S2-specific mAb also failed to detect expression of either full-length or degraded spike protein in cells infected with VacV-S-Ii, whereas both the full-length and cleaved S2 domain of spike were detected in cells infected with VacV-S (Fig. 6B). Similarly, we were also unable to detect expression of the Ii in cells infected with VacV-S-Ii (Fig. 6C). In contrast, Ii conjugated to the gp$_{61–80}$ I-A^b–restricted peptide from the LCMV glycoprotein was expressed in cells infected with VacV-Ii-gp$_{61–80}$, which confirms our previous finding demonstrating the utility of using VacV-expressing Ii conjugated to peptide Ags (32). Thus, these data show that a C-terminal conjugation of Ii to full-length SARS-CoV-2 spike fails to produce a stable chimeric Ag in vitro.
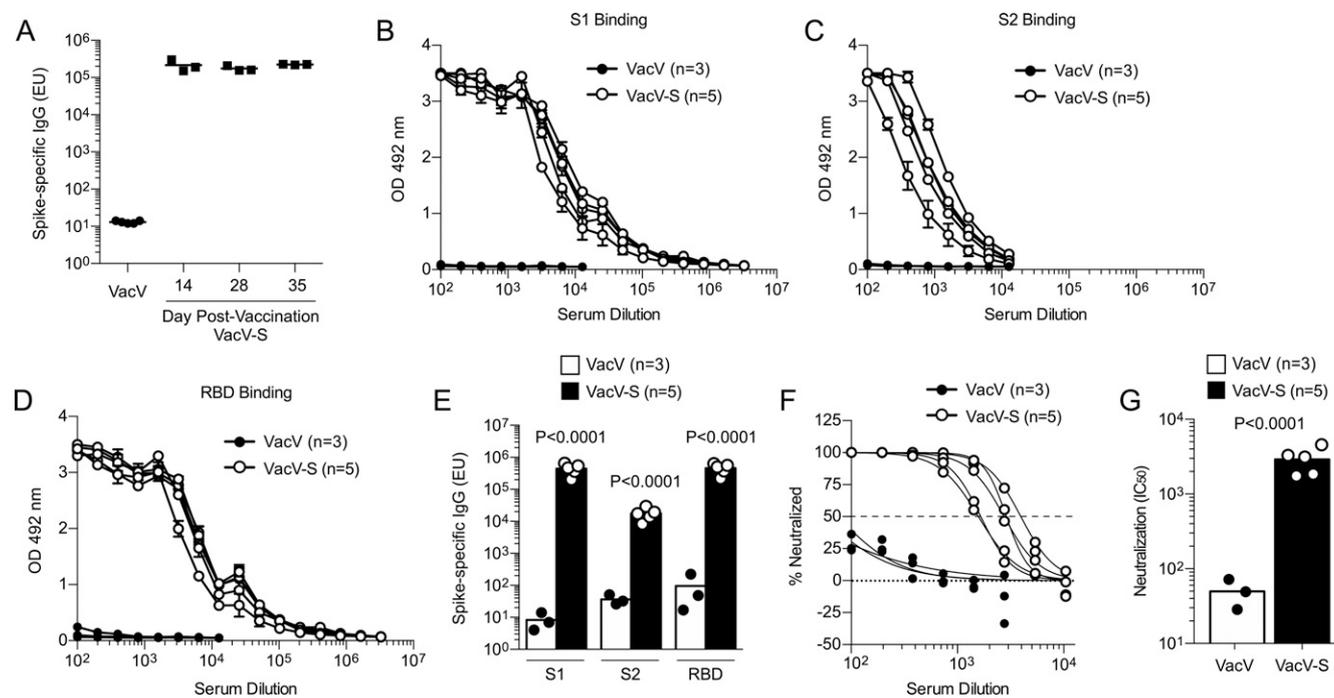
FIGURE 5. S-specific IgG-neutralizing Abs form following vaccination with VacV-S. (**A**) Naive C57BL/6 mice were immunized with 1×10^7 PFU VacV or VacV-S. S-specific Abs were quantified in the serum on the indicated day postimmunization. (**B–D**) Serum from mice immunized as in (A) was tested for reactivity to the (B) S1 domain, (C) S2 domain, or (D) RBD of SARS-CoV-2 spike following serial dilution. (**E**) Quantification of end point titers for data shown in (B)–(D). (**F**) Percentage of neutralization of a pseudotyped VSV-expressing SARS-CoV-2 spike using serum from immunized animals. (**G**) Calculation of IC_{50} of serum from (F). Error bars in (B)–(D) indicate the range of technical replicates ran in duplicate, and each line represents serum dilutions obtained from an individual animal. Data are representative of serum collected from two independent experiments.

To determine whether VacV-S-Ii would promote the activation of $CD8^+$ or $CD4^+$ T cells in vivo, mice were vaccinated with VacV, VacV-S, or VacV-S-Ii, and IFN-γ following peptide stimulation was analyzed in the spleen on day 7 postvaccination. We found that conjugating spike to Ii resulted in reduced activation of both S1- and S2-specific $CD8^+$ T cells in vivo, whereas expansion of B8R-specific $CD8^+$ T cells was similar (Fig. 6D–G). Interestingly, we observed no significant difference in the activation of S1-specific $CD4^+$ T cells in mice vaccinated with VacV-S compared with VacV-S-Ii (Fig. 6H), suggesting that despite our inability to detect high expression of S-Ii in vitro, there was sufficient Ag expressed to activate helper $CD4^+$ T cells in vivo. Similarly, S-specific IgG Abs could also be detected in animals immunized with VacV-S-Ii, although at significantly lower levels compared with the VacV-S immunization (Fig. 6I). Thus, these data demonstrate that although conjugating Ii to Ags can result in stronger cellular immune responses in some instances, conjugating spike to Ii resulted in destabilization and reduced expression of the full-length chimeric Ag in vitro and did not promote stronger cellular or humoral immune responses in vivo.

Discussion

The emergence of COVID-19 has caused substantial morbidity and mortality within the global population, and the development of a broadly distributed, effective vaccine will be necessary to end the current pandemic. Our findings in this study show that recombinant VacV expressing the native, full-length version of SARS-CoV-2 spike is highly immunogenic. In fact, the magnitude of the S-specific $CD8^+$ T cell response was nearly as large as that observed against the native H2-K^b–restricted B8R$_{20–27}$ peptide, which is one of the strongest antiviral $CD8^+$ T cell responses that has been documented in C57BL/6 mice (42). Interestingly, we also found that both the cellular and humoral

immune response generated against spike after VacV-S immunization primarily targeted the S1 domain, which is in contrast to observations in humans, in which the majority of the defined T cell epitopes following SARS-CoV-1 infections have been found primarily in the S2 domain of spike (43). This suggests that either more immunodominant epitopes in mice are found within the S1 domain or the possibility that during natural coronavirus infection, the adaptive immune response is diverted away from epitopes within the S1 domain and that expression of spike by recombinant VacV could be an effective strategy to generate protective immunity against this critical portion of the viral Ag in vivo. Whether cellular immunity, humoral immunity, or the combination of both will be necessary to provide the level of immunological protection necessary to neutralize and prevent SARS-CoV-2 infections within the human population remains to be fully elucidated.

It remains unclear whether a strong memory T cell response against SARS-CoV-2 will be necessary to provide protective immunity in humans. Notably, both Ag-specific $CD8^+$ and $CD4^+$ T cells have been shown to provide protection against SARS-CoV-1 in mouse models (44–47), and the quantity of neutralizing Abs against SARS-CoV-1 following vaccination did not directly correlate with protection in ferrets (48). Studies have also recently found that long-lived SARS-CoV-2–specific memory $CD8^+$ T cells can be identified in only approximately half of COVID-19 survivors and that $CD4^+$ T cell responses seem to dominate in most patients (49). Elderly COVID-19 patients exhibit impaired activation and function of $CD8^+$ T cells (50), which may suggest that limited cytotoxic responses mounted against the virus following infection could be an underlying cause for increased morbidity and mortality within this highly susceptible population. Studies analyzing the S-specific T cell response in human ACE2 transgenic mice (51) infected with SARS-CoV-2 or VacV-S immunization should reveal whether the
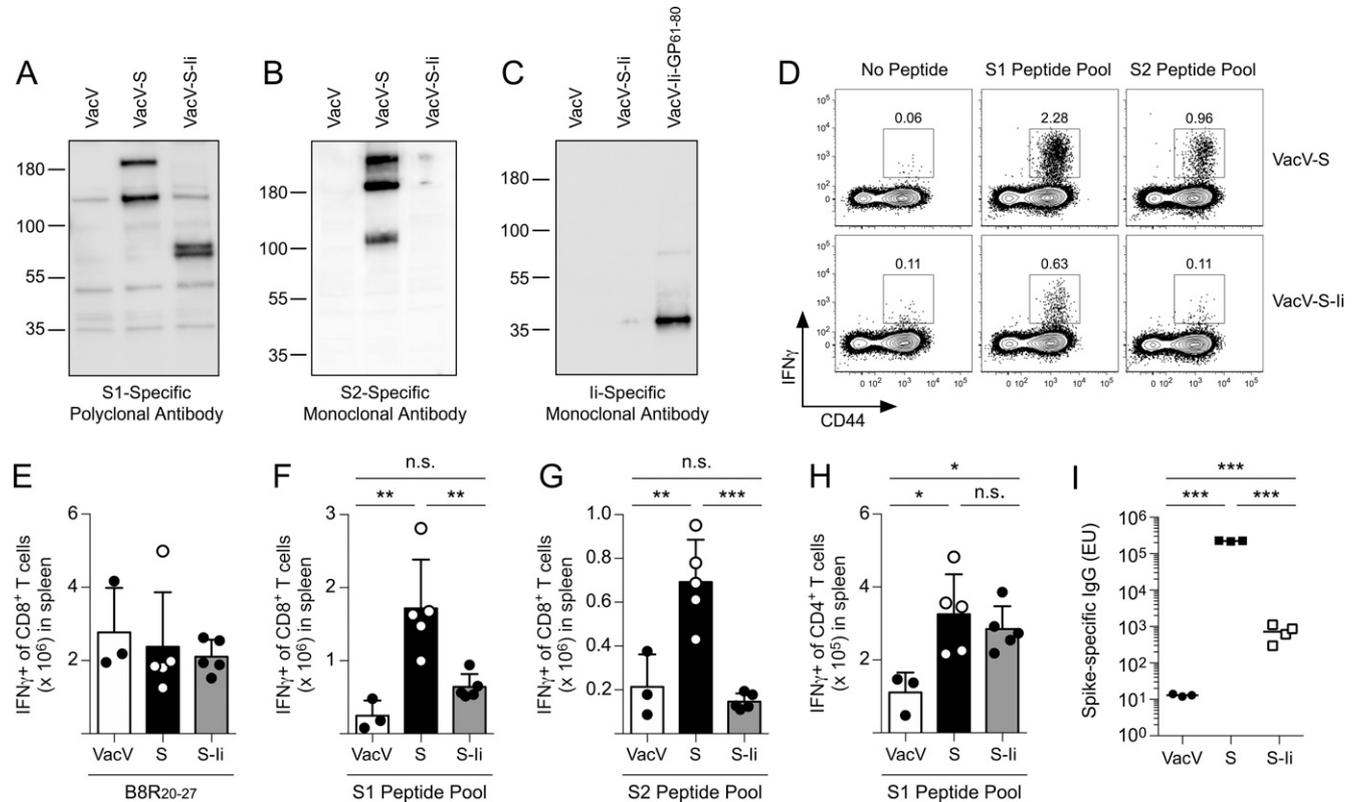
FIGURE 6. VacV-S-Ii does not elicit stronger immune responses than VacV-S. (**A–C**) BSC-40 cells were infected with VacV, VacV-S, VacV-S-Ii, or VacV-Ii-gp$_{61-80}$ (MOI = 1.0). Twenty-four hours later, expression of (A) spike using an S1-specific polyclonal Ab, (B) spike using an S2-specific mAb, and (C) MHC-II Ii was analyzed by immunoblot. (**D**) Naive C57BL/6 mice were immunized with 1×10^7 PFU of VacV-S or VacV-S-Ii. On day 7 postvaccination, splenocytes were stimulated with S1 or S2 peptide pools, and IFN-γ expression was analyzed by intracellular stain. (**E–G**) Number of IFN-γ^+ CD8$^+$ T cells in the spleen following stimulation with (E) B8R$_{20-27}$, (F) S1 peptides, or (G) S2 peptides. (**H**) Number of IFN-γ^+ CD4$^+$ T cells following stimulation with S1 peptides. (**I**) Spike-specific IgG was quantified on day 35 postimmunization with VacV, VacV-S, or VacV-S-Ii. Error bars indicate SD of the mean, and data are representative of two independent experiments using three to five mice per group. $*p < 0.05$, $**p < 0.01$, $***p < 0.001$.

breadth and/or magnitude of Ag-specific memory T cells that form following immunization are similar or are more diverse and robust when compared with the natural viral infection and whether S-specific memory CD8$^+$ or CD4$^+$ T cells are necessary or sufficient to provide protective immunity against SARS-CoV-2 infection.

Although mRNA and adenovirus (Ad)–vectored vaccines have emerged as the early leaders in the battle against COVID-19, efforts to develop and optimize alternative vaccination strategies should continue as the long-term efficacy of current, emergency use–authorized mRNA- and Ad vector–based vaccines to prevent this infection remains unknown (52). In addition, the development of neutralizing Abs against SARS-CoV-2 often requires two consecutive administrations of the COVID-19 mRNA vaccines (53, 54), whereas we demonstrate the generation of neutralizing Abs following a single immunization with VacV-S. Unlike what has been found in many patients who have recovered from COVID-19 (49), we observed the development of a strong cytotoxic T cell response in mice that readily persisted following VacV-S immunization, particularly against the S1 domain of spike. This finding agrees with other vaccination studies using animal models, in which immunization with either MVA-S, recombinant Ad (serotype 5)–expressing spike, or the spike mRNA vaccine (mRNA-1273) all elicited the generation of more S-specific cytotoxic CD8$^+$ T cells that produced IFN-γ following stimulation with S1 peptides than when stimulated with S2 peptides (29, 30, 55, 56), suggesting that delivery of this viral Ag in the context of a vaccine results in strong activation of S1-specific cellular immunity. There is also the potential that immunological memory elicited by the COVID-19 mRNA vaccinations may

diminish over time, and subsequent booster immunizations may be required (57). Heterologous booster immunizations using recombinant viral vectors expressing spike could be one appealing approach as this strategy is known to specifically and rapidly boost cellular immunity (58). In fact, a heterologous prime-boost regimen using a DNA-based vaccine followed by immunization with MVA-S elicited stronger T cell responses in mice compared with two subsequent immunizations with MVA-S (29), suggesting that delivery of spike by VacV or MVA could significantly boost both the cytotoxic and helper T cell responses in individuals that have previously received the COVID-19 mRNA-based vaccine(s).

Although we and others have reported that conjugation of the MHC-II Ii to peptide Ags enhanced T cell activation in vivo (31–33), we found this not to be true when conjugated to the C terminus of the full-length spike protein from SARS-CoV-2. In fact, our data suggest that this chimeric Ag (S-Ii) became highly unstable, was unable to activate CD8$^+$ T cells in vivo, and S-specific Ab formation was compromised compared with immunization with VacV expressing the full-length, native version of spike. As mentioned previously, MVA expressing full-length spike has also been shown to be effective at generating S-specific Abs in vivo that could neutralize SARS-CoV-2 (30). Similar to our findings, those Abs also primarily targeted the S1 domain and RBD of spike. In contrast, immunization with MVA expressing a secreted version of the S1 domain of spike generated a stronger cytotoxic CD8$^+$ T cell response compared with MVA expressing full-length spike but failed to produce Abs that could neutralize SARS-CoV-2 in vitro (30). Overall, these findings suggest that recombinant VacV or MVA vectors

expressing the full-length, native version of spike from betacoronaviruses is an effective strategy to promote strong cellular and humoral immunity against this viral Ag.

Disclosures

The authors have no financial conflicts of interest.

References

1. Wiersinga, W. J., A. Rhodes, A. C. Cheng, S. J. Peacock, and H. C. Prescott. 2020. Pathophysiology, transmission, diagnosis, and treatment of coronavirus disease 2019 (COVID-19): a review. *JAMA.* 324: 782–793.
2. Hu, B., H. Guo, P. Zhou, and Z.-L. Shi. 2021. Characteristics of SARS-CoV-2 and COVID-19. *Nat Rev Microbiol.* 19: 141–154
3. Su, S., G. Wong, W. Shi, J. Liu, A. C. K. Lai, J. Zhou, W. Liu, Y. Bi, and G. F. Gao. 2016. Epidemiology, genetic recombination, and pathogenesis of coronaviruses. *Trends Microbiol.* 24: 490–502.
4. de Wit, E., N. van Doremalen, D. Falzarano, and V. J. Munster. 2016. SARS and MERS: recent insights into emerging coronaviruses. *Nat. Rev. Microbiol.* 14: 523–534.
5. Fontanet, A., and S. Cauchemez. 2020. COVID-19 herd immunity: where are we? *Nat. Rev. Immunol.* 20: 583–584.
6. V'Kovski, P., A. Kratzel, S. Steiner, H. Stalder, and V. Thiel. 2020. Coronavirus biology and replication: implications for SARS-CoV-2. *Nat. Rev. Microbiol.* 19: 155–170
7. Letko, M., A. Marzi, and V. Munster. 2020. Functional assessment of cell entry and receptor usage for SARS-CoV-2 and other lineage B betacoronaviruses. *Nat. Microbiol.* 5: 562–569.
8. Liu, L., P. Wang, M. S. Nair, J. Yu, M. Rapp, Q. Wang, Y. Luo, J. F. Chan, V. Sahi, A. Figueroa, et al. 2020. Potent neutralizing antibodies against multiple epitopes on SARS-CoV-2 spike. *Nature.* 584: 450–456.
9. Chi, X., R. Yan, J. Zhang, G. Zhang, Y. Zhang, M. Hao, Z. Zhang, P. Fan, Y. Dong, Y. Yang, et al. 2020. A neutralizing human antibody binds to the N-terminal domain of the Spike protein of SARS-CoV-2. *Science.* 369: 650–655.
10. Ejemel, M., Q. Li, S. Hou, Z. A. Schiller, J. A. Tree, A. Wallace, A. Amcheslavsky, N. Kurt Yilmaz, K. R. Buttigieg, M. J. Elmore, et al. 2020. A cross-reactive human IgA monoclonal antibody blocks SARS-CoV-2 spike-ACE2 interaction. *Nat. Commun.* 11: 4198.
11. Chi, X., X. Liu, C. Wang, X. Zhang, X. Li, J. Hou, L. Ren, Q. Jin, J. Wang, and W. Yang. 2020. Humanized single domain antibodies neutralize SARS-CoV-2 by targeting the spike receptor binding domain. *Nat. Commun.* 11: 4528.
12. Wec, A. Z., D. Wrapp, A. S. Herbert, D. P. Maurer, D. Haslwanter, M. Sakharkar, R. K. Jangra, M. E. Dieterle, A. Lilov, D. Huang, et al. 2020. Broad neutralization of SARS-related viruses by human monoclonal antibodies. *Science.* 369: 731–736.
13. Sattler, A., S. Angermair, H. Stockmann, K. M. Heim, D. Khadzhynov, S. Treskatsch, F. Halleck, M. E. Kreis, and K. Kotsch. 2020. SARS-CoV-2-specific T cell responses and correlations with COVID-19 patient predisposition. *J. Clin. Invest.* 130: 6477–6489.
14. Le Bert, N., A. T. Tan, K. Kunasegaran, C. Y. L. Tham, M. Hafezi, A. Chia, M. H. Y. Chng, M. Lin, N. Tan, M. Linster, et al. 2020. SARS-CoV-2-specific T cell immunity in cases of COVID-19 and SARS, and uninfected controls. *Nature.* 584: 457–462.
15. Peng, Y., A. J. Mentzer, G. Liu, X. Yao, Z. Yin, D. Dong, W. Dejnirattisai, T. Rostron, P. Supasa, C. Liu, et al; Oxford Immunology Network Covid-19 Response T cell Consortium; ISARIC4C Investigators. 2020. Broad and strong memory CD4$^+$ and CD8$^+$ T cells induced by SARS-CoV-2 in UK convalescent individuals following COVID-19. *Nat. Immunol.* 21: 1336–1345.
16. Karlsson, A. C., M. Humbert, and M. Buggert. 2020. The known unknowns of T cell immunity to COVID-19. *Sci. Immunol.* 5: eabe8063.
17. Stewart, A. J., and P. M. Devlin. 2006. The history of the smallpox vaccine. *J. Infect.* 52: 329–334.
18. Esparza, J., A. Nitsche, and C. R. Damaso. 2018. Beyond the myths: novel findings for old paradigms in the history of the smallpox vaccine. *PLoS Pathog.* 14: e1007082.
19. Hammarlund, E., M. W. Lewis, S. G. Hansen, L. I. Strelow, J. A. Nelson, G. J. Sexton, J. M. Hanifin, and M. K. Slifka. 2003. Duration of antiviral immunity after smallpox vaccination. *Nat. Med.* 9: 1131–1137.
20. Hammarlund, E., M. W. Lewis, J. M. Hanifin, M. Mori, C. W. Koudelka, and M. K. Slifka. 2010. Antiviral immunity following smallpox virus infection: a case-control study. *J. Virol.* 84: 12754–12760.
21. Kim, S. H., S. G. Yeo, K. H. Park, J. W. Bang, H. B. Kim, N. J. Kim, Y. Jee, H. Cho, M. D. Oh, and K. W. Choe. 2007. The persistence of humoral and cellular immunities more than three decades after smallpox vaccination. *Clin. Microbiol. Infect.* 13: 91–93.
22. Amanna, I. J., M. K. Slifka, and S. Crotty. 2006. Immunity and immunological memory following smallpox vaccination. *Immunol. Rev.* 211: 320–337.
23. Koch, T., C. Dahlke, A. Fathi, A. Kupke, V. Krähling, N. M. A. Okba, S. Halwe, C. Rohde, M. Eickmann, A. Volz, et al. 2020. Safety and immunogenicity of a modified vaccinia virus Ankara vector vaccine candidate for Middle East respiratory syndrome: an open-label, phase 1 trial. *Lancet Infect. Dis.* 20: 827–838.
24. Kreijtz, J. H., M. Goeijenbier, F. M. Moesker, L. van den Dries, S. Goeijenbier, H. L. De Gruyter, M. H. Lehmann, G. Mutsert, D. A. van de Vijver, A. Volz, et al. 2014. Safety and immunogenicity of a modified-vaccinia-virus-Ankara-based influenza A H5N1 vaccine: a randomised, double-blind phase 1/2a clinical trial. *Lancet Infect. Dis.* 14: 1196–1207.
25. Sebastian, S., and S. C. Gilbert. 2016. Recombinant modified vaccinia virus Ankara-based malaria vaccines. *Expert Rev. Vaccines* 15: 91–103.
26. Pérez, P., M. Q. Marín, A. Lázaro-Frías, N. J. de Oya, A.-B. Blázquez, E. Escribano-Romero, C. Ó. S. Sorzano, J. Ortego, J.-C. Saiz, M. Esteban, et al. 2018. A vaccine based on a modified vaccinia virus Ankara vector expressing Zika virus structural proteins controls Zika virus replication in mice. *Sci. Rep.* 8: 17385.
27. Bisht, H., A. Roberts, L. Vogel, A. Bukreyev, P. L. Collins, B. R. Murphy, K. Subbarao, and B. Moss. 2004. Severe acute respiratory syndrome coronavirus spike protein expressed by attenuated vaccinia virus protectively immunizes mice. *Proc. Natl. Acad. Sci. USA.* 101: 6641–6646.
28. Kitabatake, M., S. Inoue, F. Yasui, S. Yokochi, M. Arai, K. Morita, H. Shida, M. Kidokoro, F. Murai, M. Q. Le, et al. 2007. SARS-CoV spike protein-expressing recombinant vaccinia virus efficiently induces neutralizing antibodies in rabbits pre-immunized with vaccinia virus. *Vaccine.* 25: 630–637.
29. García-Arriaza, J., U. Garaigorta, P. Pérez, A. Lázaro-Frías, C. Zamora, P. Gastaminza, C. Del Fresno, J. M. Casasnovas, C. Ó. S. Sorzano, D. Sancho, and M. Esteban. 2021. COVID-19 vaccine candidates based on modified vaccinia virus Ankara expressing the SARS-CoV-2 spike protein induce robust T- and B-cell immune responses and full efficacy in mice. *J. Virol.* DOI: 10.1128/JVI.02260-20.
30. Routhu, N. K., N. Cheedarla, S. Gangadhara, V. S. Bollimpelli, A. K. Boddapati, A. Shiferaw, S. A. Rahman, A. Sahoo, V. V. Edara, L. Lai, et al. 2021. A modified vaccinia Ankara vector-based vaccine protects macaques from SARS-CoV-2 infection, immune pathology, and dysfunction in the lungs. *Immunity.* 54: 542–556.e9.
31. Holst, P. J., M. R. Sorensen, C. M. Mandrup Jensen, C. Orskov, A. R. Thomsen, and J. P. Christensen. 2008. MHC class II-associated invariant chain linkage of antigen dramatically improves cell-mediated immunity induced by adenovirus vaccines. *J. Immunol.* 180: 3339–3346.
32. Hobbs, S. J., J. C. Harbour, P. A. Yates, D. Ortiz, S. M. Landfear, and J. C. Nolz. 2020. Vaccinia virus vectors targeting peptides for MHC class II presentation to CD4$^+$ T cells. *Immunohorizons.* 4: 1–13.
33. Esposito, I., P. Cicconi, A. M. D'Alise, A. Brown, M. Esposito, L. Swadling, P. J. Holst, M. R. Bassi, M. Stornaiuolo, F. Mori, et al; PEACHI Consortium. 2020. MHC class II invariant chain-adjuvanted viral vectored vaccines enhances T cell responses in humans. *Sci. Transl. Med.* 12: eaaz7715.
34. Wyatt, L. S., P. L. Earl, and B. Moss. 2015. Generation of recombinant vaccinia viruses. *Curr. Protoc. Mol. Biol.* 39: 14A.4.1–14A.4.18.
35. Schnell, M. J., J. E. Johnson, L. Buonocore, and J. K. Rose. 1997. Construction of a novel virus that targets HIV-1-infected cells and controls HIV-1 infection. *Cell.* 90: 849–857.
36. Lawson, N. D., E. A. Stillman, M. A. Whitt, and J. K. Rose. 1995. Recombinant vesicular stomatitis viruses from DNA. *Proc. Natl. Acad. Sci. USA.* 92: 4477–4481.
37. Case, J. B., P. W. Rothlauf, R. E. Chen, Z. Liu, H. Zhao, A. S. Kim, L.-M. Bloyet, Q. Zeng, S. Tahan, L. Droit, et al. 2020. Neutralizing antibody and soluble ACE2 inhibition of a replication-competent VSV-SARS-CoV-2 and a clinical isolate of SARS-CoV-2. *Cell Host Microbe.* 28: 475–485.e5.
38. Oguntuyo, K. Y., C. S. Stevens, C. T. Hung, S. Ikegame, J. A. Acklin, S. S. Kowdle, J. C. Carmichael, H. P. Chiu, K. D. Azarm, G. D. Haas, et al. 2021. Quantifying absolute neutralization titers against SARS-CoV-2 by a standardized virus neutralization assay allows for cross-cohort comparisons of COVID-19 sera. *mBio* 12: e02492-20.
39. Ferrara, F., and N. Temperton. 2018. Pseudotype neutralization assays: from laboratory bench to data analysis. *Methods Protoc.* 1: 8.
40. Samji, T., and K. M. Khanna. 2017. Understanding memory CD8$^+$ T cells. *Immunol. Lett.* 185: 32–39.
41. Schröder, B. 2016. The multifaceted roles of the invariant chain CD74–more than just a chaperone. *Biochim. Biophys. Acta* 1863: 1269–1281.
42. Tscharke, D. C., G. Karupiah, J. Zhou, T. Palmore, K. R. Irvine, S. M. Haeryfar, S. Williams, J. Sidney, A. Sette, J. R. Bennink, and J. W. Yewdell. 2005. Identification of poxvirus CD8+ T cell determinants to enable rational design and characterization of smallpox vaccines. *J. Exp. Med.* 201: 95–104.
43. Ahmed, S. F., A. A. Quadeer, and M. R. McKay. 2020. Preliminary identification of potential vaccine targets for the COVID-19 coronavirus (SARS-CoV-2) based on SARS-CoV immunological studies. *Viruses.* 12: 254.
44. Channappanavar, R., C. Fett, J. Zhao, D. K. Meyerholz, and S. Perlman. 2014. Virus-specific memory CD8 T cells provide substantial protection from lethal severe acute respiratory syndrome coronavirus infection. *J. Virol.* 88: 11034–11044.
45. Zhao, J., J. Zhao, A. K. Mangalam, R. Channappanavar, C. Fett, D. K. Meyerholz, S. Agnihothram, R. S. Baric, C. S. David, and S. Perlman. 2016. Airway memory CD4(+) T cells mediate protective immunity against emerging respiratory coronaviruses. *Immunity.* 44: 1379–1391.

46. Zhao, J., J. Zhao, and S. Perlman. 2010. T cell responses are required for protection from clinical disease and for virus clearance in severe acute respiratory syndrome coronavirus-infected mice. *J. Virol.* 84: 9318–9325.

47. Channappanavar, R., J. Zhao, and S. Perlman. 2014. T cell-mediated immune response to respiratory coronaviruses. *Immunol. Res.* 59: 118–128.

48. See, R. H., M. Petric, D. J. Lawrence, C. P. Y. Mok, T. Rowe, L. A. Zitzow, K. P. Karunakaran, T. G. Voss, R. C. Brunham, J. Gauldie, et al. 2008. Severe acute respiratory syndrome vaccine efficacy in ferrets: whole killed virus and adenovirus-vectored vaccines. *J. Gen. Virol.* 89: 2136–2146.

49. Dan, J. M., J. Mateus, Y. Kato, K. M. Hastie, E. D. Yu, C. E. Faliti, A. Grifoni, S. I. Ramirez, S. Haupt, A. Frazier, et al. 2021. Immunological memory to SARS-CoV-2 assessed for up to 8 months after infection. *Science.* 371: eabf4063.

50. Westmeier, J., K. Paniskaki, Z. Karaköse, T. Werner, K. Sutter, S. Dolff, M. Overbeck, A. Limmer, J. Liu, X. Zheng, et al. 2020. Impaired cytotoxic CD8$^+$ T cell response in elderly COVID-19 patients. [Published erratum appears in 2020 *mBio.* 11: e02805-20.] *mBio.* 11: e02243-20.

51. McCray, P. B., Jr., L. Pewe, C. Wohlford-Lenane, M. Hickey, L. Manzel, L. Shi, J. Netland, H. P. Jia, C. Halabi, C. D. Sigmund, et al. 2007. Lethal infection of K18-hACE2 mice infected with severe acute respiratory syndrome coronavirus. *J. Virol.* 81: 813–821.

52. Pardi, N., M. J. Hogan, F. W. Porter, and D. Weissman. 2018. mRNA vaccines - a new era in vaccinology. *Nat. Rev. Drug Discov.* 17: 261–279.

53. Widge, A. T., N. G. Rouphael, L. A. Jackson, E. J. Anderson, P. C. Roberts, M. Makhene, J. D. Chappell, M. R. Denison, L. J. Stevens, A. J. Pruijssers, et al; mRNA-1273 Study Group. 2021. Durability of responses after SARS-CoV-2 mRNA-1273 vaccination. *N. Engl. J. Med.* 384: 80–82.

54. Walsh, E. E., R. W. Frenck, Jr., A. R. Falsey, N. Kitchin, J. Absalon, A. Gurtman, S. Lockhart, K. Neuzil, M. J. Mulligan, R. Bailey, et al. 2020. Safety and immunogenicity of two RNA-based Covid-19 vaccine candidates. *N. Engl. J. Med.* 383: 2439–2450.

55. Feng, L., Q. Wang, C. Shan, C. Yang, Y. Feng, J. Wu, X. Liu, Y. Zhou, R. Jiang, P. Hu, et al. 2020. An adenovirus-vectored COVID-19 vaccine confers protection from SARS-COV-2 challenge in rhesus macaques. *Nat. Commun.* 11: 4207.

56. Corbett, K. S., D. K. Edwards, S. R. Leist, O. M. Abiona, S. Boyoglu-Barnum, R. A. Gillespie, S. Himansu, A. Schäfer, C. T. Ziwawo, A. T. DiPiazza, et al. 2020. SARS-CoV-2 mRNA vaccine design enabled by prototype pathogen preparedness. *Nature.* 586: 567–571.

57. Feldman, R. A., R. Fuhr, I. Smolenov, A. M. Ribeiro, L. Panther, M. Watson, J. J. Senn, M. Smith, Ö. Almarsson, H. S. Pujar, et al. 2019. mRNA vaccines against H10N8 and H7N9 influenza viruses of pandemic potential are immunogenic and well tolerated in healthy adults in phase 1 randomized clinical trials. *Vaccine.* 37: 3326–3334.

58. Nolz, J. C., and J. T. Harty. 2011. Strategies and implications for prime-boost vaccination to generate memory CD8 T cells. *Adv. Exp. Med. Biol.* 780: 69–83.